EFFECTS OF BORON OXIDE ADDITION ON DIELECTRIC PROPERTIES OF LOW LOSS STEATITE CERAMICS

ZİYA ASLANOGLU[#], HÜSEYİN Ş. SOYKAN*, ZEHRA ERDEM**, ERDOGAN ŞENTURK**

Superates Refractory Inc. Maslak Mah. Maslak Ayazağa Cad. No:9 34398 Sisli/Istanbul, Turkey
*Marzinc Marmara Geri Kazanım A.Ş., Barbaros Bulvarı No:93B Beşiktaş/İstanbul, Turkey
**Sakarya University, Dept. of Physics, 54100, Sakarya, Turkey

[#]Corresponding author, e-mail: zaslanoglu@yahoo.com

Steatite ceramics have been fabricated by using starting materials such as talc, clay, and barium carbonate with addition of boron oxide (B_2O_3). B_2O_3 has been found to be a useful flux to densify MgO–Al_2O_3–SiO_2–BaO (MASB) powders. The steatite ceramic with a relative density of 97% was obtained at a sintering temperature of 1200 °C. The effects of B_2O_3 additions on the dielectric properties of the samples have been investigated. Doping with B_2O_3 significantly affects the dielectric properties. The values of dielectric properties of the samples changes with B_2O_3 addition. This may be attributed to the quartz phase. Hence, a ceramic with lower dielectric loss was obtained for use in high temperature electrical applications.

INTRODUCTION

Steatite ceramics are inorganic materials made from natural raw materials containing predominantly magnesium silicate and can be considered in place of alumina as a cost-effective way to meet performance requirements. The steatite ceramics are widely used in electronics, electrical engineering, radio electronics, and other fields owing to their low dielectric losses, high temperature resistance, and high mechanical strength [1-3].

The steatite ceramics are formulated from a natural raw material containing magnesium silicate, known as talc together with additions of clay and flux. Electrical properties of steatite ceramics were investigated several years. Different additives (ZnO, Al_2O_3) have been investigated regarding to their effects on dielectric properties [4]. The type of flux influences the electrical characteristics and leads to the following differentiation: steatite for low-frequency, normal steatite, as well as special steatite with low loss factor.

The steatite ceramics are usually produced by using talc (about 80 to 90 %), plastic clay (about 5 to 10 %) and a fluxmelting agent (about 5 to 10 %). During the preparation of the mass, low quantities of clay and/ or barium carbonate are added. The material is fired at around 1400°C and it is formed by crystallization, fusion and dissolving during the vitrification. Typical steatite materials have the following analysis: 58 – 65 % SiO_2, 26-32 % MgO, 3-6 % Al_2O_3, 1.3 % Na_2O. Typically 7-10 % BaO is added to obtain low-loss steatite. The structure of steatite phase consists of about 70 % of crystalline $MgSiO_3$ (so-called Protoenstatite) and of about 30% of glass phase [5]. It has an impervious material structure that has good mechanical strength, and low dielectric loss. It makes excellent insulators for radio frequency applications, and exhibits high volume resistivity up to 1000°C [6-7].

The sintering aids were usually used to improve the sinterability of steatite ceramics made from natural material. For this purpose, B_2O_3 was used as a sintering aid due to its low melting point and less harmful effect on the insulating characteristics than other sintering aids [8-9]. In the present study, the effects of B_2O_3 addition on the dielectric properties of steatite ceramics were investigated.

EXPERIMENTAL

Talc, clay and barium carbonate were used as starting materials. Starting materials were weighed to get a commercial grade low-loss steatite composition. Different ratios of B_2O_3 (0, 0.25, 0.75, and 1.5 wt.%) were added to the mixture in the form of boric acid (H_3BO_3), respectively and indicated as MASB0, MASB5,

MASB10 and MASB20. The materials were dry pressed and then sintered at 1200°C for 2 hours in air atmosphere. The detailed experimental procedure was given in elsewhere [10-11].

Dielectric properties were characterized by Complex Dielectric Spectroscopy (CDS) which is a powerful technique for investigating the dielectric properties of samples used in solid state. The sintered pellets were gently cleaned, polished. Then, the surfaces of the pellets were electroded with silver paste. The dimensions of the electrodes were ~10x1 mm^3 with an inter-electrode distance of ~1 mm. Dielectric properties of the sample were studied with a Hawlett-Packert 4194A Impedance/Gain-Phase Analyzer in the frequency range from 1 kHz-40 MHz. The complex dielectric constant $\varepsilon^*(w) = \varepsilon`(w) - i\varepsilon``(w)$ [$\varepsilon`(w)$ is the real part of dielectric constant and $\varepsilon``(w)$ is the lost part) were carried out in room temperature. At least, 100 different frequencies applied in logarithmic scale for the samples.

RESULTS AND DISCUSSION

The X-ray diffraction patterns of MASB20 steatite powders with different sintering temperatures are shown in Figure 1. After sintering at 1000°C, protoenstatite phase was observed with quartz, aluminum silicate, and barium aluminum silicate phases. The characteristic peaks are (212) and (310) of protoenstatite phase were identified. Crystallization of protoenstatite phase increased with addition of B$_2$O$_3$. During sintering, talc decomposes and gives a mixture of fine-grained protoenstatite crystals in a silica matrix at about 1000 °C. As similar
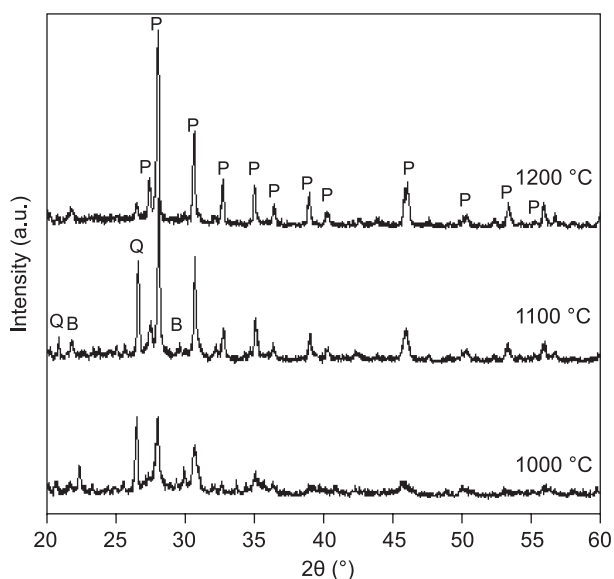

Figure 1. X-ray diffraction patterns of MASB20 steatite ceramics were sintered at different temperatures. (P - protoenstatite; Q - quartz; B - barium aluminum silicate; A - aluminum silicate).

to talc, clay decomposes at 980°C to form fine-grained mullite in a silica matrix. This process is accompanied by production of free silica or quartz. The quartz grains are undesirable constituents of steatite and must be eliminated [11]. The crystallization rate of protoenstatite phase and appearance of other crystalline phases were also dependent to sintering temperature. Highest crystallization rate of protoenstatite was obtained with MASB20 samples. After sintering at 1100°C for MASB20 samples, aluminum silicate and barium aluminum silicate dissolved into the glassy matrix and disappeared. Although the peak intensities of protoenstatite phase increased, there was still a minor quartz phase. However, the crystallization rate of protoenstatite reached a maximum value at sintering temperature of 1200°C [10]. At this temperature, quartz phase disappeared and only a single protoenstatite crystalline phase was obtained. The process of protoenstatite crystallization in talc generally starts at temperatures above 1250°C and fully develops at 1420°C [11,12]. It is clear that the addition of B$_2$O$_3$ accelerates the crystallization of protoenstatite at lower temperatures.

Microstructural investigations were also conducted on sintered samples by Scanning Electron Microscope (SEM). Large pores were occurred in sintered samples without B$_2$O$_3$ addition. As natural process, visible cracks also developed in steatite body. After B$_2$O$_3$ addition, pore elimination and enhancement of densification for MASB20 samples were promoted by the viscous flow B$_2$O$_3$ addition and hence, a nearly dense ceramic was obtained [11]. Easier densification of MASB specimens with B$_2$O$_3$ addition may be due to the flux effect of B$_2$O$_3$ which enhances the densification during sintering. Because of the low melting point of B$_2$O$_3$, the procedure of sintering MASB ceramics would be a reactive liquid-phase sintering process. With liquid formation, there was a densification, even at low sintering temperatures such as 1000°C, due to capillary force exerted by the liquid on the particles, while actual sintering temperature was around 1400°C for steatite ceramics [10,13].

The real part of dielectric constant was calculated from the equation $\varepsilon` = Cd/\varepsilon_0 A$, where ε_0 is the permittivity of free space. The dielectric loss $\varepsilon``$ was calculated from the equation $\varepsilon`` = \varepsilon`tg\delta$, where $\delta = 90 - \Phi$ and Φ is the phase angle. The variation of the frequency dependence of the real part of dielectric constant at some DC voltages (at room temperature) of steatite with the addition of B$_2$O$_3$ in different concentration (0, 0.25, 0.75, and 1.5 wt.%) were investigated. The dielectric constant of the samples MASB0 and MASB20 as a function of frequency were shown in Figure 2.

It is clear from the figure that $\varepsilon`(w)$ decreases nonlinearly with frequency for each sample. The decrease in $\varepsilon`(w)$ with frequency can be attributed to the fact that, at low frequencies, $\varepsilon`(w)$ for polar materials depends on the contribution of multicomponents of polarizability, deformational (electronic and ionic) and relaxation

(orientational and interfacial) polarization. The former polarizability depends on the electrons and ions while the latter depends on orientational or interfacial effects. The increase in frequency leads to a decrease in orientational polarization, since this takes more time than electronic and ionic polarization. Such a decrease tends to reduce the value of ε` with increasing frequency, reaching a constant value at higher frequency [14].

As it seen in Figure 2a and 2b, there are some fluctuations in dielectric constants at beginning of the external applied voltages (0-20 V) and then it disappears at high frequencies. All dielectric constants with different voltages remain stable at 100 kHz and higher frequencies except for MASB20. When increasing frequencies up to 100 kHz, all dielectric constants start to remain stable at approximately 6. MASB20 reaches this value at lower frequencies than 100 kHz. This critical value shows expire of electronic mechanism.

In addition, dielectric constants vary with the frequency and external applied voltages (5, 10 and 20 Volt). Dielectric constants were affected slightly with increasing voltages. There is a non-linear decreasing of dielectric constant with increasing voltages at constant frequency but for the all samples, increasing frequencies up to 100 kHz were causes a step type increase in dielectric constant. Moreover, none of the samples were show any relaxation behavior under applied voltages. This result may reveal that possible and much more relaxation might occur at lower or higher frequencies.

The loss factor of dielectric constant shown as $\tan\delta = \varepsilon`` / \varepsilon`$, where $\varepsilon``$ is imaginary part of dielectric constant and and $\tan\delta$ is dielectric loss. The frequency dependence of the dielectric loss of samples MASB0 and MASB20 were shown in Figure 3. All samples show that dielectric loss is decreasing with increasing frequency. Similar to the real part of dielectric constant
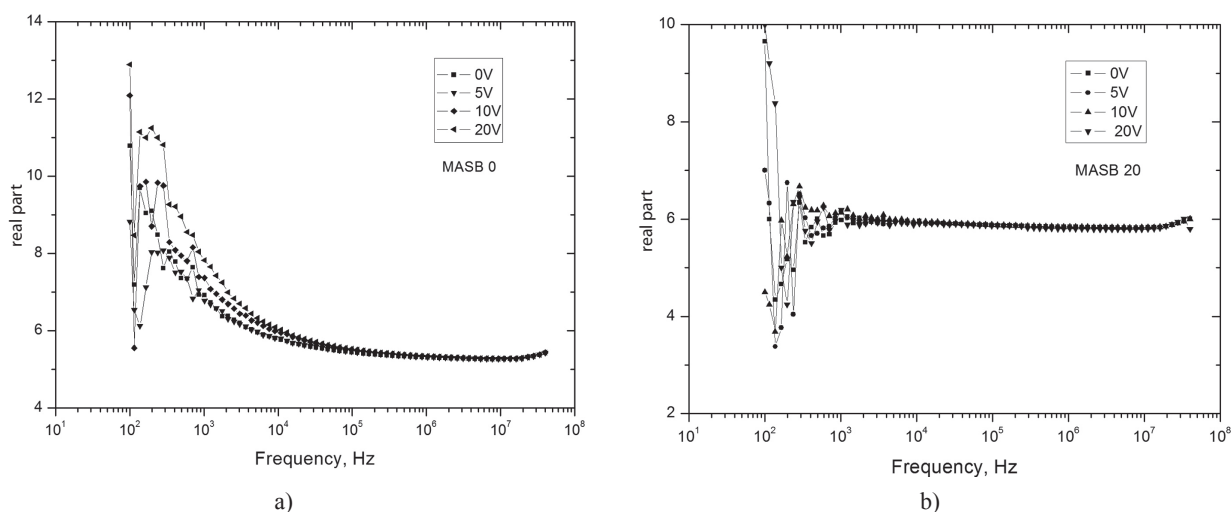

a)

b)

Figure 2. The dielectric constant of the samples MASB0 (a) and MASB20 (b) as a function of frequency.
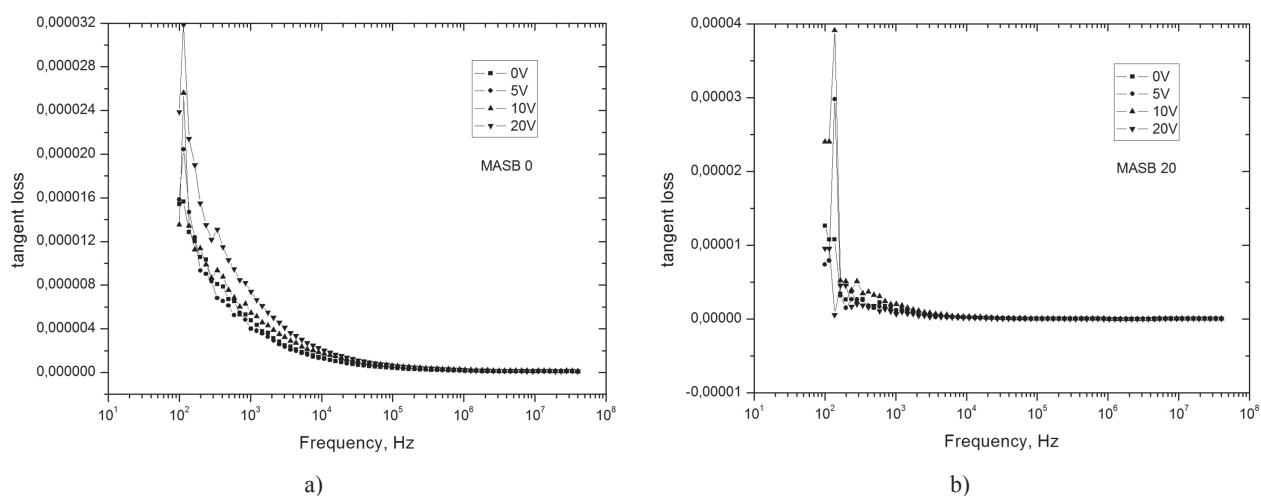

a)

b)

Figure 3. Frequency dependence of the dielectric loss of samples MASB0 (a) and MASB20 (b).

for all samples, there is no any change in loss factor with applied voltages after 100 kHz frequency. The behavior of loss factors in different voltages looks like step type.

The loss factor for all samples in the range of applied voltages and frequencies is between 10^{-5} and 10^{-6}. Thus, it can be said that loss factor of all samples are very low. Accordingly, the interaction of applied electromagnetic waves with samples results in very little energy lost. Also, there is no relaxation loss in the examined frequency range similar to the reel part of dielectric constant. Especially MASB20 sample were show that very low tangent loss in large frequency region which is reveal that this is superior properties for industrial applications.

The AC conductivity shows a typical power law behavior and increases in mentioned frequency interval. The frequency dependence of the AC conductivity is given by the relation;

$$\sigma(w) = \sigma_o + Aw^s \tag{1}$$

where A and s are constants. Here σ_o is called DC conductivity and it is independent from frequency. However, this part of measured samples is not seen because it remains in lower frequency. However, the estimated values, obtained from the experimental results fit into the equation (1), are given in Table 1.

Table 1. Characteristic values obtained from fitted experimental results to the theoretical expression.

Series	σ_o (S/m)	A	s
MASB 0	5×10^{-8}	10^{-10}	0.68
MASB 5	9×10^{-7}	9×10^{-10}	0.61
MASB 10	1×10^{-8}	10^{-8}	0.45
MASB 20	3×10^{-8}	10^{-11}	0.75

The frequency dependent exponent, s, is a characteristic parameter and dimensionless. It depends on the material temperature and applied frequency. The index is generally less than or close to to unity. The variation of s with temperature gives the conductivity mechanism in the sample examined [15]. The variations of conductivity properties of steatite with the addition of B_2O_3 in different concentrations are depicted in Figure 4. It is clearly seen from the figure that the conductivity extremely depends on the addition of B_2O_3. It is noteworthy that small amount of the addition firstly results in increasing on the conductivity and then vice versa. The characteristic parameters obtained from the fitted experimental results to equation (1) with B_2O_3 content were shown in Figure 5.

Figure 5 shows the variations of dielectric properties with the B_2O_3 additions. However, the real part of dielectric constant increases between MASB0 and MASB5 then decreases until MASB20 for a specific frequency. The same trend was observed for the loss factor. Figure 4 shows numerical values of the frequency

dependence of the loss factor. It is clear from the figure that the loss factor has very low values for MASB20. It ranges from 0.084 (for 1 kHz) to 0.0045 (for 10 MHz). Therefore, a steatite with lower dielectric loss was obtained.

It is interesting that the electrical properties (real part of the dielectric constant, dielectric loss and conductivity) of the samples with addition of B_2O_3 firstly deteriorated for the concentration ranging from 0 to 0.25 and then improved ranging from 0.25 to 1.5. According to previous reports, the dielectric properties was simultaneously affected by many factors, mainly caused not only by the lattice vibration modes, but also by densification, pores, grain sizes/boundaries, and secondary phases [16,17]. Therefore, the mentioned dielectric properties above may be attributed to these effects. A shifting from decreasing to increasing in dielectric properties may be attributed to the quartz phase. The increased amount of B_2O_3 addition results in
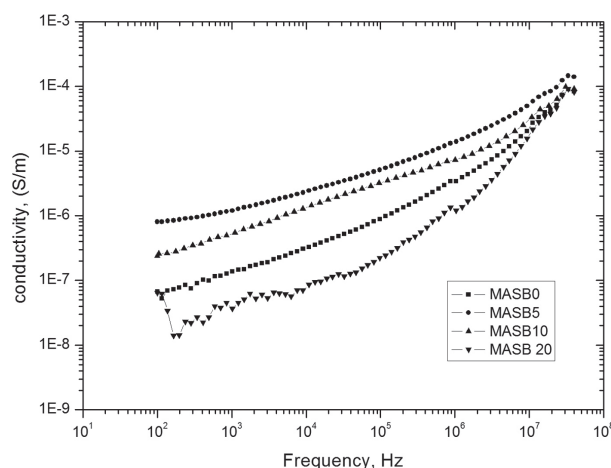

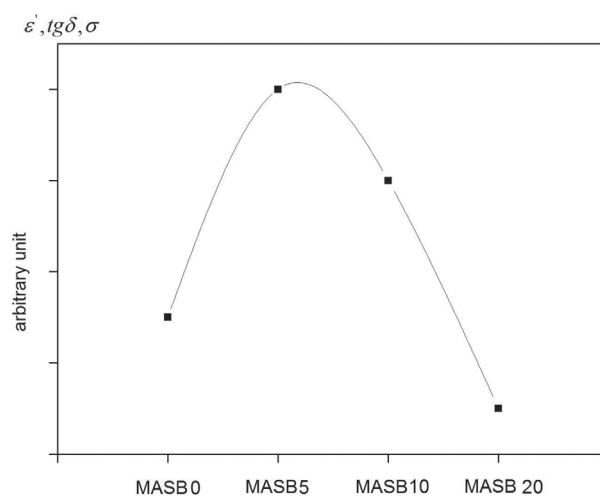
Figure 4. Frequency dependence of the conductivity.

Figure 5. The variations of the dielectric properties of the samples contatining the additions.

disappearing of quartz phase for MASB10 and MASB20 samples. This may be due to the fact that quartz dissolves into the glassy matrix and disappears for MASB 10 and MASB20 samples.

CONCLUSIONS

By using B_2O_3 additions, a nearly dense ceramic can be obtained at a lower sintering temperature than that of industrial practice. The addition of B_2O_3 in different concentrations clearly affects the dielectric properties of samples. The dielectric properties of the samples shift clearly an increasing trend in a specific concentration (0.25). This behavior may be attributed to the quartz phase of the samples. In addition, the loss factor for all samples in the range of applied voltages and examined frequencies is between 10^{-5} and 10^{-6} .This is very low value and it has probability to use in electrical applications. With increasing frequency, a non-linear decrease was observed in the real part of dielectric constant and dielectric losses. These are independent from voltage and frequency after 100 kHz and also these are shows step like change in increasing voltages.

References

1. Kingery W. D., Bowen H. K., Uhlmann D. R.: *Introduction to Ceramics*, p.307, Wiley&Sons, New York, , 1976.
2. Kharitonov F., Shapiro L. E.: Glass and Ceramics *46*, 162 (1989).
3. Kulkarni A. K., Dalvi P. Y., Barde M. L.: Trans. of Powder Metallurgy Assoc. of India *17*, 101 (1990).
4. Zonov A. V., Kharitonov F. Y.: Glass Ceram. (Engl. Transl.) *44*, 1 (1987).
5. Takher E. A., Fedoseeva T. I., Kellerman V. Y., Popilskii R.: Glass and Ceramics *31*, 108 (1974).
6. Tripathi U. C., Agrawal G. N., Joshi V. C.: Trans. of the Indian Ceramic Soc. *37*, 179 (1978).
7. Avetikov, V. G., Borisova, A. Y. U., Zinko, E.: Glass and Ceramics, *27*, 5-6, 294-296 (1970).
8. Sumi K., Kobayashi Y., Kato E.: J. Am. Ceram. Soc. *82*, 783 (1999).
9. Luo L.H., Zhou H., Xu C.: J. Mat. Sci. Mat. Elec. *12*, 371 (2001).
10. Soykan H. S.: Ceramics International *33*, 911 (2007).
11. Soykan H. S., Aslanoglu Z., Karakas Y.: Adv. Applied Ceramics *105*, 270 (2006).
12. Mielcarek W., Nowak-Wozny D., Prociow K.: J. Eur. Ceram. Soc. *24*, 3817 (2004).
13. Yang C. F., Cheng C. M.: Ceramics International *25*, 383 (1999).
14. Farid A. M., Atyia H. E., Hegab N.A.: Vacuum *80*, 284 (2005).
15. El-Barry A. M. A., Atyia H. E.: Physica B *368*, 1 (2005).
16. Kim W. S., Hong H. T., Kim E. S., Yoon K. H.: Jpn. J. Appl. Phys. *37*, 5367 (1998).
17. Cheng-Liang H., Cheng-Shing H.: Materials Research Bulletin *36*, 2677 (2001).